Cellulose
https://doi.org/10.1007/s10570-020-03210-w

ORIGINAL RESEARCH

Synthesis of microcrystalline cellulose/TiO_2/fluorine/styrene-acrylate coatings and the application for simulated paper cultural relic protection

Jicheng Xu · Tao Zhang · Yan Jiang · Qian Chen · Dongya Yang · Fengxian Qiu · Zongping Yu

Received: 8 January 2020 / Accepted: 2 May 2020

Abstract Paper cultural relics are prone to embrittlement, yellowing, powdering, mildew and damage due to the brittleness of materials, natural deterioration, microbial corrosion, and man-made destruction. To prolong the expected life of paper cultural relics, a series of novel microcrystalline cellulose/TiO_2/fluorine/styrene-acrylate coatings were prepared with modified microcrystalline cellulose, modified nano-TiO_2, dodecafluoroheptyl methacrylate, and several acrylate monomers. The prepared coatings were analyzed by infrared spectroscopy, transmission electron microscopy, UV–Vis spectroscopy, and performance-testing devices. In addition, the optimized protective coatings were coated on the simulated paper cultural relic surface, and its protective effects were evaluated by tensile strength retention rate and weight loss rate. When the content of modified nano-TiO_2 was 1.0 wt%, the protective coatings exhibited good hydrophobicity, oil repellency, mechanical strength, anti-aging, and reversibility.

J. Xu · Y. Jiang
Zhenjiang Key Laboratory of Functional Chemistry, Institute of Chemistry and Materials Science, Zhenjiang College, Zhenjiang 212028, China

J. Xu · T. Zhang (✉) · Q. Chen · D. Yang · F. Qiu (✉)
Institute of Green Chemistry and Chemical Technology, School of Chemistry and Chemical Engineering, Jiangsu University, Zhenjiang 212013, China
e-mail: zhangtaochem@163.com

F. Qiu
e-mail: fxqiu@ujs.edu.cn

Z. Yu
Suzhou Mingda Macromolecule Science and Technology Co., Ltd., Suzhou 215234, China

Published online: 18 May 2020

Graphic abstract

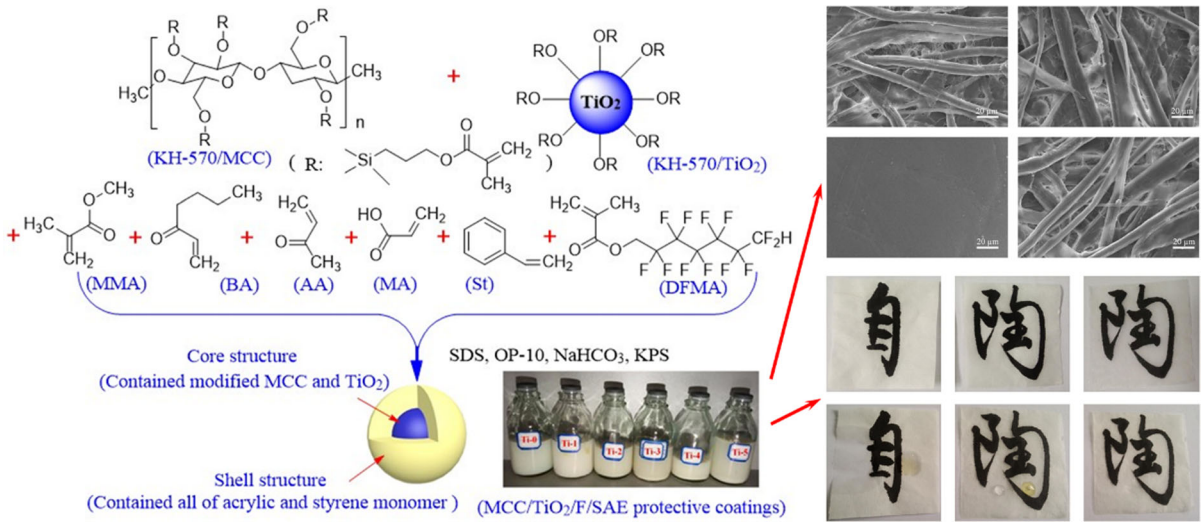

Keywords Paper cultural relics · Microcrystalline cellulose · Dry heat accelerated aging · Nano-TiO_2

Introduction

Cultural relics of various materials, which are the legacies of ancestors for social and economic activities, have significant historical, artistic and scientific value (Liu et al. 2019; Xu et al. 2018a, b). Paper cultural relics are the most important and largest number of cultural relics related to the splendid ancient civilization of humankind. They have high value for the future of all countries and include calligraphy and painting, books, newspapers, archives, maps, banknotes, etc. However, thousands of paper cultural relics are aged and damaged annually, and the degree of aging becomes more and more severe as time goes on (Xu et al. 2020b). The primary components of paper cultural relics are cellulose, lignin, and hemicelluloses, and its aging has three main factors (Chen et al. 2016; Zervos and Alexopoulou 2015). Firstly, cellulose is easily hydrolyzed and oxidized in the nature environment, leading to the aging of paper cultural relics. As the acidic conditions can promote the hydrolysis of cellulose, various acids are not conducive to the protection of paper cultural relics, such as acids produced by photooxidation and oxidation, inorganic acids in the air, organic acids produced by microorganisms (Bicchieri and Sodo 2016). Secondly, cellulose can be destroyed by various types of bacteria and mildew (Kim et al. 2015). The growth of fungi on the paper will ruin the paper sizing, causing the degradation of paper mechanical properties and the formation of stains (Pfendler et al. 2019; Sterflinger 2010). Lastly, the excessive ultraviolet radiation and artificial lighting, extremes of temperatures and humidity, and human factors would accelerate the aging of paper cultural relics.

Many countries have developed measures to prevent further aging of paper cultural relics, such as mounting methods, low temperature deworming techniques (Melo et al. 2019), plasma deacidification methods (Li et al. 2014b), and electrospinning techniques (Li et al. 2014a). However, these above methods often suffer from the disadvantages, such as high cost, poor mechanical properties and hydrophobicity, which limiting the scope of its application. In recent years, resin coating protection technology is to apply high-quality resin coating on the surface of paper to form a protective film (Wang et al. 2019). At the same time, the resin can penetrate the inside of paper to strengthen the fibers. Therefore, resin coating has attracted high interest as an excellent candidate for paper cultural relics protection owing to its good sealing effect, waterproof, oil-proof, anti-fouling, and anti-ultraviolet properties (Xu et al. 2020a).

As a natural green polymer, microcrystalline cellulose (MCC) is widely used in the textile,

pharmaceutical, food, cosmetic, and chemical industries due to its rich material sources, biodegradability, low cost, renewable, and good mechanical properties (Jun et al. 2017; Li et al. 2019; Qiu et al. 2020). The hydroxyl groups in MCC can form new hydrogen bonds with cellulose in paper to increase the degree of polymerization, improve the compatibility of the protective coatings, and enhance the mechanical properties of paper (Ashori and Nourbakhsh 2010; Zhang et al. 2019). However, MCC has a relatively strong polar surface and poor dispersibility in a non-polar solvent. Therefore, MCC should be modified with γ-methacryloxypropyl trimethoxysilane (KH-570) to obtain better dispersibility and hydrophobicity. Nano-TiO_2 has been paid much attention in practical applications such as environmental purification (Kalu et al. 2019), sterilization (MacFarlane et al. 2011), self-cleaning (Giolando 2016), and UV resistance (Wang et al. 2016). However, excess nano-TiO_2 particles tend to agglomerate and affect the transparency of the polymer emulsion and film. Therefore, the amount of nano-TiO_2 needs to be controlled within a specific range and modified by a silane coupling agent to improve its dispersibility (López-Zamora et al. 2018; Purcar et al. 2019). Fluorine can impart excellent performances to polymer, and it presents hydrophobicity, lipophobicity, chemical resistance, stain resistance, and remarkable resistance to environmental degradation compared with their non-fluorinate analogues (Yang et al. 2016; Zhang et al. 2016b). Dodecafluoroheptyl methacrylate (DFMA) is usually used as a polymerized monomer to improve polymer performance due to its polymerizable double bonds and high concentrations of fluorine atoms. Therefore, the preparation of the fluorine-containing polystyrene acrylate coating can maintain the extraordinary performance of polystyrene acrylate and fluoropolymers (Li et al. 2015; Zhang et al. 2016a).

In this study, novel paper cultural relic protective coatings were synthesized by semi-continuous seed emulsion and pre-emulsification polymerization methods with modified MCC, modified nano-TiO_2, DFMA, and several acrylate monomers. The physical properties of emulsions including appearance, stability, viscosity, and surface tension were investigated. The hydrophobicity, acid/alkali resistance, mechanical properties, and contact angle of coating films were measured. Also, after coating the preferred protective coatings on the simulated paper cultural relics, the effects of the dry heat accelerated aging test and reversibility experiment were carefully studied and analyzed.

Experimental

Materials

DFMA was purchased from Harbin Xuejia Fluorine-Silicon Chemical Co., Ltd., Haerbin, China. Sodium dodecyl sulfate (SDS) was acquired from Shanghai Reagent Factory, Shanghai, China. Potassium persulfate (KPS) was provided by Tianjin Chemical Reagent Factory, Tianjin, China. Nano-TiO_2 (Rutile titanium dioxide, average grain size: 14 nm) was purchased from Shanghai Jianghu Industrial Co., Ltd., Shanghai, China. All other reagents were purchased from Sinopharm Chemical Reagent Co., Ltd., Shanghai, China.

Preparation of simulated paper cultural relics

Xuan paper is a Chinese handmade paper widely used in traditional painting and calligraphy. Hongxing brand Xuan paper (obtained from Beijing Xuan Paper Co., Ltd., China) was selected for the experiments. To better investigate the changes of the paper sample, Chinese characters were written on the surface of Xuan paper to simulate paper cultural relics.

Paper was sampled and coated according to the methods of Chinese National Standards GB/T 450-2008 and GB 7691-2003, respectively. Sample-A was a paper sample without protective coatings. Sample-B was some parts of Sample-A after being coated with protective coatings by RDS #12 wire rod coater (RD Specialties Inc, USA) and hung to dry at room temperature.

Preparation of modified MCC (KH-570/MCC)

The MCC was added into the deionized water, activated by ultrasonic (40 kHz, 35 W) for 24 h, then filtered, washed, and vacuum dried. This step was to break the hydrogen bonds in MCC and enhance its reactivity. The above obtained activated MCC and 95 wt% ethanol was mixed by ultrasonic (40 kHz, 35 W) until dispersed uniformly. Then KH-570 (m_{KH-570}:m_{MCC} = 8:100) was added and reacted for 2 h at

80 °C. Finally, the KH-570/MCC was prepared after the mixture was filtered, washed, and vacuum dried. The synthetic route of KH-570/MCC is shown in Fig. 1.

Preparation of modified nano-TiO_2 (KH-570/TiO_2)

The nano-TiO_2 was modified using KH-570 as a coupling agent to improve its suspension in water-based systems. KH-570 and ethanol ($V_{C_2H_5OH} : V_{H_2O} = 1:9$)

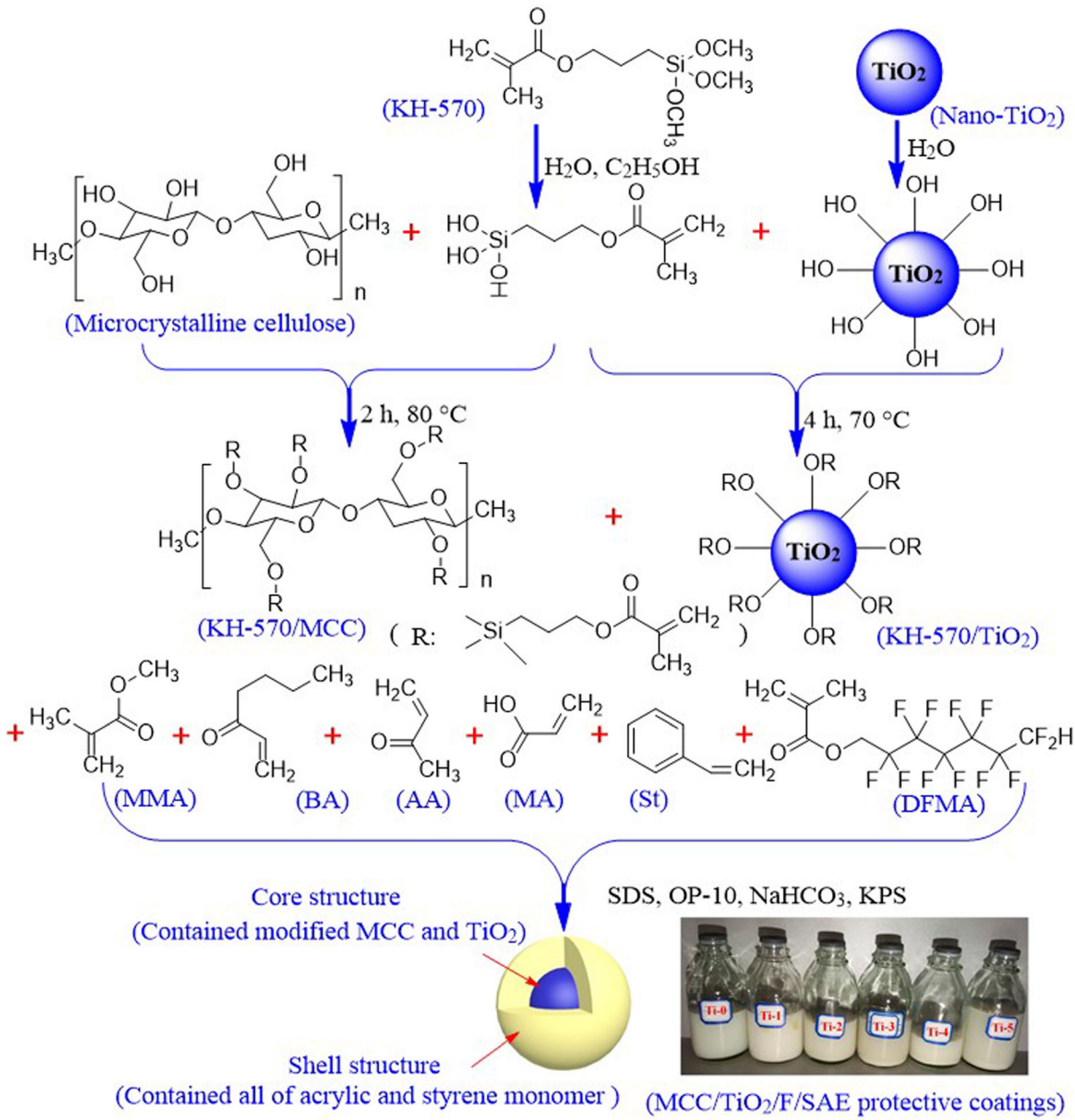

Fig. 1 The synthetic routes of KH-570/MCC, KH-570/TiO_2 and MCC/TiO_2/F/SAE protective coatings

were mixed under ultrasound for 0.5 h, then nano-TiO_2 was added and mixed for 0.5 h. The pH of the mixture was adjusted to 9–10 with NaOH. The reaction was carried out for 4 h at 70 °C. After centrifugation and vacuum dried, the KH-570/TiO_2 was prepared. The synthetic route of KH-570/TiO_2 is shown in Fig. 1.

Preparation of microcrystalline cellulose/TiO_2/fluorine/styrene-acrylate (MCC/TiO_2/F/SAE) protective coatings

1. The first step: Compound emulsifier was obtained by mixing OP-10 (polyoxyethylene (10) octylphenyl ether) and SDS with a mass ratio of 2:1. Two-thirds of compound emulsifier and distilled water were added into the four-necked round flask and stirred vigorously until completely dissolved. After the above mixture was heated to 50 °C, a certain amount of DFMA, methyl methacrylate (MMA), butyl acrylate (BA), acrylic acid (AA), methacrylic acid (MA), and styrene (St) was added, and then reacted for 1 h with stirring. The shell pre-emulsion was prepared.
2. The second step: The remaining compound emulsifier was added into another four-necked flask, then KH-570/MCC and KH-570/TiO_2 were added and stirred for 1 h at 50 °C. The core pre-emulsion was prepared.
3. The third step: One-third of the initiator (KPS) and the buffer solution ($NaHCO_3$) were added into the above core pre-emulsion mixture. After the mixture was heated to 80 °C, one-ninth of the prepared shell pre-emulsion was added. Until the blue phase of the mixture appeared, one-third of KPS was added dropwise. Simultaneously, the remaining shell pre-emulsion was added drop by drop slowly within 2 h. At the end of the dropwise addition, the remaining of KPS was added. The emulsion was further reacted at 90 °C for 4 h, and then cooled with stirring at room temperature. Finally, $NH_3{\cdot}H_2O$ was used to adjust pH to 7-8, and the MCC/TiO_2/F/SAE protective coatings with core–shell structure were prepared. According to the contents of KH-570/TiO_2 (0, 0.25 wt%, 0.50 wt%, 0.75 wt%, 1.00 wt%, and 1.25 wt% of the total mass of other monomers), the coatings were expressed as Ti-0, Ti-1, Ti-2, Ti-3, Ti-4, and Ti-5, respectively. The detailed synthetic route and recipes of MCC/TiO_2/F/SAE protective coatings are shown in Fig. 1 and Table 1, respectively.

The MCC/TiO_2/F/SAE protective coating emulsions were coated on the polytetrafluoroethylene plates and dried at room temperature to obtain films. Then, the protective coating films were placed in sealed bags for future research.

Characterization

The characterization of protective coatings

The protective coating emulsions were sealed at room temperature and protected from light for more than 6 months to evaluate its storage stability. The emulsion was cooled to − 20 °C for 18 h and then placed at 25 °C for 6 h to investigate the freeze–thaw stability. All experiments were repeated 5 times (the experiments below are the same). The emulsion was placed in a vacuum drying oven at 60 °C for 72 h to measure the high-temperature stability.

The apparent viscosity and surface tension of emulsions were measured by an NDJ-9S numerical viscometer (Shanghai Precision and Scientific Instrument Co., Ltd., China) and a DCAT 11 surface/interfacial tension tester (Dataphysics, Germany), respectively. All reported values were the average of five measurements (the tests below are the same).

Fourier transform infrared (FT-IR) spectrum was tested by an Avatar 360 Nicolet FT-IR spectrometer (Madison, USA). UV–Vis spectrum was obtained on a UV-2450 UV–Vis spectrometer (Shimadzu, Japan). The morphology of emulsion was investigated by a Tecnai 12 transmission electron microscopy (Philips, Netherlands) at 120 kV.

The protective coating films were cut into 2 × 2 cm squares, weighed (marked as m_1) and immersed in deionized, 3.0% NaOH and 3.0% H_2SO_4 at room temperature to measure the swelling degree (ω). After soaking for 24 h, the films were taken out from the test solution, and the surface was wiped with filter paper and weighed (marked as m_2) again. The ω of the film was calculated by the following formula (1):

Table 1 The detailed polymerization recipes of MCC/TiO_2/F/SAE protective coatings

Sample	Ti-0	Ti-1	Ti-2	Ti-3	Ti-4	Ti-5
KH-570/TiO_2 (g)	0	0.07	0.14	0.21	0.28	0.35
KH-570/MCC (g)	0	1.62	1.62	1.62	1.62	1.62
DFMA (g)	0	5.02	5.02	5.02	5.02	5.02
St (g)	4.20	4.20	4.20	4.20	4.20	4.20
MMA (g)	2.23	2.23	2.23	2.23	2.23	2.23
MA (g)	1.85	1.85	1.85	1.85	1.85	1.85
BA (g)	11.50	11.50	11.50	11.50	11.50	11.50
AA (g)	0.32	0.32	0.32	0.32	0.32	0.32
OP-10 (g)	0.42	0.72	0.72	0.72	0.72	0.72
SDS (g)	0.21	0.36	0.36	0.36	0.36	0.36
KPS (g)	0.13	0.17	0.17	0.17	0.17	0.17
$NaHCO_3$ (g)	0.10	0.13	0.13	0.13	0.13	0.13

$$\omega = \frac{m_2 - m_1}{m_1} \times 100\% \quad (1)$$

The hardness and tensile strength of films were carried out with a KYLX-A sclerometer and a KY-8000A tensile tester (Jiangdu Kaiyuan Test Machine Co., Ltd., China). The water contact angle of the film was obtained using a CAM200 optical system (KSV Instruments, Finland). The decomposition of the film was investigated by thermogravimetric analysis (TGA) using an STA 449C instrument (Netzsch, Germany) at a heating rate of 10 °C/min from room temperature to 990 °C.

The characterization of paper samples

The thickness of sample was measured by a Mitutoyo 342-251 micrometer caliper (Mitutoyo, Japan). The surface morphology of paper samples was observed using an S-4800 scanning electron microscope (Hitachi, Japan).

According to the dry heat accelerated aging method of Chinese National Standards GB/T 464-2008, the Sample-A and Sample-B were hanged in a constant temperature oven, heated for 72 h at 105 ± 2 °C. Compared to paper samples before and after the accelerated aging test, the tensile strength retention rate (u) and the weight loss rate ($\triangle m$) were calculated. The tensile strength of the paper samples before and after the aging test (marked as Y_1 and Y_2, respectively) was tested by a KY-8000A tensile tester. The u was calculated with the following formula (2):

$$u = \frac{Y_2}{Y_1} \times 100\% \quad (2)$$

The mass of paper samples before the aging test was marked as m_3, and after the aging test was marked as m_4. The $\triangle m$ was calculated with the following formula (3):

$$\Delta m = \frac{m_3 - m_4}{m_3} \times 100\% \quad (3)$$

Reversibility experiment of protective coatings

Reversible protective material means that after being used, reversible measures can be taken to return the protected sample to its original state. In order to evaluate the reversibility of materials, the paper sample coated with the protective film was immersed in acetone for 3 h to remove the coatings, and then dried and weighed. Repeat the above operation until constant weight. The sample after the reversibility experiment was denoted as the Sample-C.

Results and discussion

The properties of MCC/TiO_2/F/SAE emulsions

The properties of the emulsion are an essential aspect of the comprehensive performance of protective coatings. The physical properties of the MCC/TiO_2/F/SAE protective coating emulsions are listed in Table 2. The appearance of pure styrene acrylic

Table 2 The physical properties of MCC/TiO_2/F/SAE emulsions

Sample	Appearance	Stability			Viscosity (mPa s)	Surface tension (mN m^{-1})
		Storage	Freeze–thaw	High-temperature		
Ti-0	Translucency, blue	Stable	Stable	Stable	16.2	35.903
Ti-1	Milkiness, blue	Stable	Stable	Stable	15.3	34.870
Ti-2	Milkiness, blue	Stable	Stable	Stable	18.1	34.381
Ti-3	Milkiness, blue	Stable	Stable	Stable	20.2	33.659
Ti-4	Milkiness, blue	Stable	Stable	Stable	24.5	33.091
Ti-5	Milkiness, blue	Precipitate	Precipitate	Precipitate	29.7	32.773

emulsion (Ti-0) was translucency and blue. After the addition of DFMA, modified MCC, and nano-TiO_2, the protective coatings became milkiness and slightly blue. After 6 months of sealed storage, all emulsions were very stable except for the partial precipitation of Ti-5 emulsion. At the same time, freeze–thaw stability and high-temperature stability tests showed that all emulsions were stable except Ti-5 emulsion. These precipitations might be caused by the excessive nano-TiO_2 agglomeration.

As well known, viscosity is in connection with the permeability of emulsion. The lower viscosity is, the better the penetrability is. In Table 2, the viscosity of emulsion was small, and ranged from 16.2 to 29.7 mPa s, meeting the requirement of cultural relic protective coatings. Furthermore, the lower surface tension of the protective emulsion, the better the wettability to the substrate, and the better the adhesion effect after curing into a film. With the addition of DFMA and the increase of KH-570/TiO_2 content, the surface tension of the emulsions decreased from 35.903 (Ti-0) to 32.773 mN m^{-1} (Ti-5). This phenomenon could be explained by the fact that the modified nano-TiO_2 and DFMA had lower surface free energy.

UV–Vis spectra of Ti-0, Ti-4 and Ti-4/Ti-0 (Ti-4 under the background of Ti-0) are shown in Fig. 2. As shown in Fig. 2, the Ti-0 emulsion had absorption peaks in the range of 280 to 320 nm, and the maximum absorption wavelength was 306.3 nm. The Ti-4 emulsion appeared absorption peaks in the range of 280 to 350 nm, and the maximum absorption wavelength was 323 nm, indicating that after the addition of the modified nano-TiO_2, the UV absorption range of the protective costing was broadened, and the UV

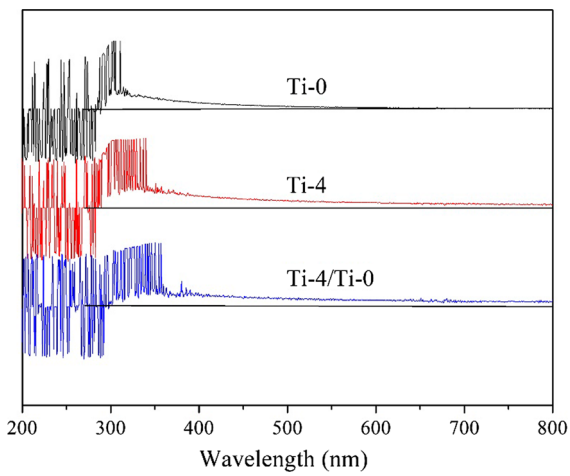

Fig. 2 UV–Vis spectra of Ti-0, Ti-4 and Ti-4/Ti-0

resistance was improved. As a comparison, the UV–Vis spectrum of the Ti-4 emulsion was scanned using a Ti-0 emulsion as a blank background. It was still found that absorption peaks of Ti-4/Ti-0 appeared in the range of 300 to 400 nm, suggesting that the modified nano-TiO_2 had UV resistance. After coating paper cultural relics with protective coatings containing modified nano-TiO_2, UV light became more challenging to reach the paper inside due to the absorption of modified nano-TiO_2. Therefore, the UV blocking performance of the coating was much improved, which could be explained by the solid band theory (Afsharpour and Hadadi 2014). In addition, it could be seen in Fig. 2 that both Ti-0 and Ti-4 had no obvious absorption peaks in the visible region. Therefore, the Ti-0 and Ti-4 emulsions had good photo-permeability, and the addition of modified nano-TiO_2 did not affect the optical performance of protective coatings.

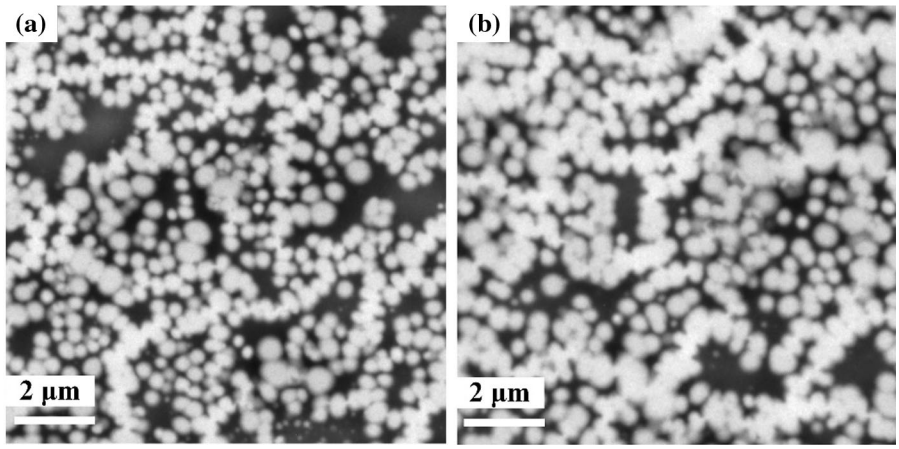

Fig. 3 TEM images of Ti-0 (**a**) and Ti-4 (**b**) emulsions

TEM images of Ti-0 (a) and Ti-4 (b) are given in Fig. 3. Figure 3 shows that all latex particles were round, indicating that the core–shell structure in the protective coatings was approximately spherical. Owing to the introduction of modified nano-TiO_2, DFMA, and modified MCC, the particle size of Ti-4 became larger than that of Ti-0. Additionally, the morphology of Ti-4 did not show any aggregation of nano-TiO_2 particles, indicating that the modified nano-TiO_2 had better compatibility.

The properties of MCC/TiO_2/F/SAE films

The protective coating films should have a complete set of comprehensive performances such as hardness, tensile strength, hydrophobic, and acid/alkaline resistance. The properties of MCC/TiO_2/F/SAE films are collected in Table 3. With the increased of the content of modified nano-TiO_2 and the addition of modified MCC and DFMA, although the hardness and tensile strength of the protective coating films increased, the swelling degree decreased. It was mainly because modified MCC with good flexibility, and rigid particle TiO_2 could be graft copolymerized with styrene acrylate by chemical bonding. Furthermore, nano-TiO_2 could shield the active groups on the surface of the film, which could prevent the film from being directly attacked by chemical reagents, thereby improving water resistance and acid/alkali resistance. Besides, the swelling degree of the film was further enhanced by adding DFMA with good water and acid/alkali resistance.

The water contact angle of the film surface can be used to characterize the hydrophobicity of the film. The larger the water contact angle, the stronger the hydrophobicity of the material (Sun et al. 2019). Figure 4 shows the water contact angle value of the MCC/TiO_2/F/SAE films. The contact angle of Ti-0 was 56.38°, but the contact angle of the other films increased gradually with the content of modified nano-TiO_2 rising. This was because the fluorine containing DFMA has hydrophobicity, and TiO_2 increased the surface roughness of the films. It is well known that the water-repellent property is enhanced by the surface

Table 3 The properties of MCC/TiO_2/F/SAE films

Sample	Hardness (HA)	Tensile strength (MPa)	Swelling degree (%)		
			NaOH (3%)	H_2SO_4 (3%)	water
Ti-0	86.1	8.39	12.8	12.4	13.7
Ti-1	86.7	12.84	11.7	8.3	10.6
Ti-2	87.3	13.81	10.9	7.6	9.5
Ti-3	87.9	14.12	10.5	6.8	8.6
Ti-4	88.6	15.67	10.1	6.3	8.3
Ti-5	89.2	16.89	9.8	5.9	8.1

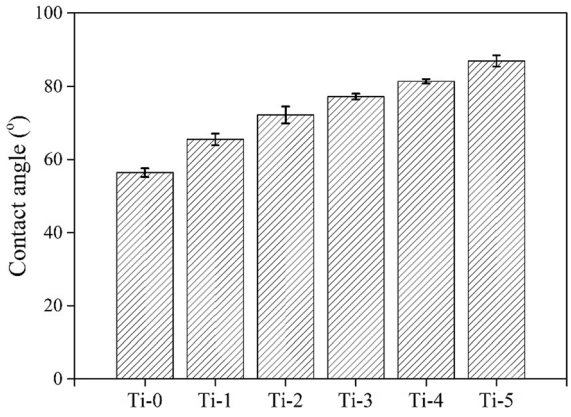

Fig. 4 The contact angle of MCC/TiO_2/F/SAE films

roughness. Therefore,the water-resistance of the films were gradually increased. This is of great useful, it may endow the protective coatings with the characteristic of hydrophobicity in the paper cultural relic protection applications.

FT-IR analysis

To investigate and compare the chemical structure of the samples, the surface functional groups of MCC (a), KH-570/MCC (b), KH-570 (c), KH-570/TiO_2 (d), Ti-0 (e), and Ti-4 (f) were analyzed by FT-IR spectra, which are shown in Fig. 5. From Fig. 5a, b, a strong absorption band of -OH stretching vibration was observed around 3200–3600 cm^{-1}. However, the -OH stretching vibration of the KH-570/MCC around 3200–3400 cm^{-1} was weaker than that of MCC, attributing to the intermolecular hydrogen bond was broken by the reaction of KH-570 and MCC. As shown in Fig. 5a, the characteristic absorption peak of β-(1,4)-two glycosides and asymmetric stretching of C–O–C was at 1052 cm^{-1} and 1115 cm^{-1}, respectively. Furthermore, the characteristic peaks appearing at 1735 cm^{-1}, 1646 cm^{-1}, and 839 cm^{-1} were ascribed to C=O, C=C, and Si–O–C, respectively. Due to overlapping absorption bands of Si–O and C–O, the absorption bands around 1150–900 cm^{-1} were indistinguishable, indicating that MCC had been successfully modified by KH-570.

Figure 5c shows that the stretching vibrations of unsaturated and saturated C–H bonds around 3100–2800 cm^{-1}, the absorption band of C=O at 1720 cm^{-1}, the peak of C=C at 1637 cm^{-1} and the characteristic peaks of Si–O–C at 1165, 1087, and 817 cm^{-1} of KH-570 were observed. The –OH stretching vibration at 3421 cm^{-1} was observed, indicating that trace amount of KH-570 had taken part in the hydrolytic reaction. In Fig. 5d, stretching vibrations of unsaturated and saturated C–H bonds around 3100-2800 cm^{-1}, absorption bands of C=O and C=C around 1730–1600 cm^{-1} were observed. Simultaneously, a sharp and broad characteristic absorption peak of Ti–O–Ti was found around 600–400 cm^{-1}, indicating that KH-570 had successfully modified TiO_2.

As can be seen from Fig. 5e, f, the peak at 1732 cm^{-1} was assigned to C=O. The stretching vibrations of saturated C–H bond around 3000–2800 cm^{-1} were found. Due to the polymerization reaction, the peak of the C=C (around 1680–1620 cm^{-1}) contained in the monomers was disappeared, suggesting that all of the monomers had reacted completely. Since the $–CF_3$ and $–CF_2–$ groups in DFMA were introduced into the coating through polymerization, the peak of Ti-4 was broader and taller than that of Ti-0 around 1300–1100 cm^{-1}. Moreover, the absorption peak of Ti-4 around 3400–3200 cm^{-1} was higher than that of Ti-0. This peak belonged to the stretching vibration of –OH groups which did not react completely, suggesting that the modified MCC had grafted successfully. The skeletal vibrations of benzene ring around 1620–1450 cm^{-1} were found in Fig. 5e, f due to the introduction of styrene. However, on account of the introduction of KH-570/TiO_2, the characteristic absorption peak of TiO_2 around 800–400 cm^{-1} covered up C–H bending vibration of the benzene ring in Fig. 5f. The above results showed that the MCC/TiO_2/F/SAE materials had been successfully prepared.

TG analysis

Thermal stability is an important parameter for cultural relic protection materials. The thermal stability of Ti-0 and Ti-4 are shown in Fig. 6. In Fig. 6, the mass loss of Ti-4 at 310 °C was 11.23% due to thermal dehydroxylation of the modified nano-TiO_2 surface. The mass loss of Ti-0 and Ti-4 was 98.02% and 95.48% at 400 °C, respectively. This was mainly because the modified nano-TiO_2 in Ti-4 did not decompose at this temperature. The decomposition temperature of Ti-4 was always higher than that of Ti-0, testifying that the introduction of DFMA and TiO_2

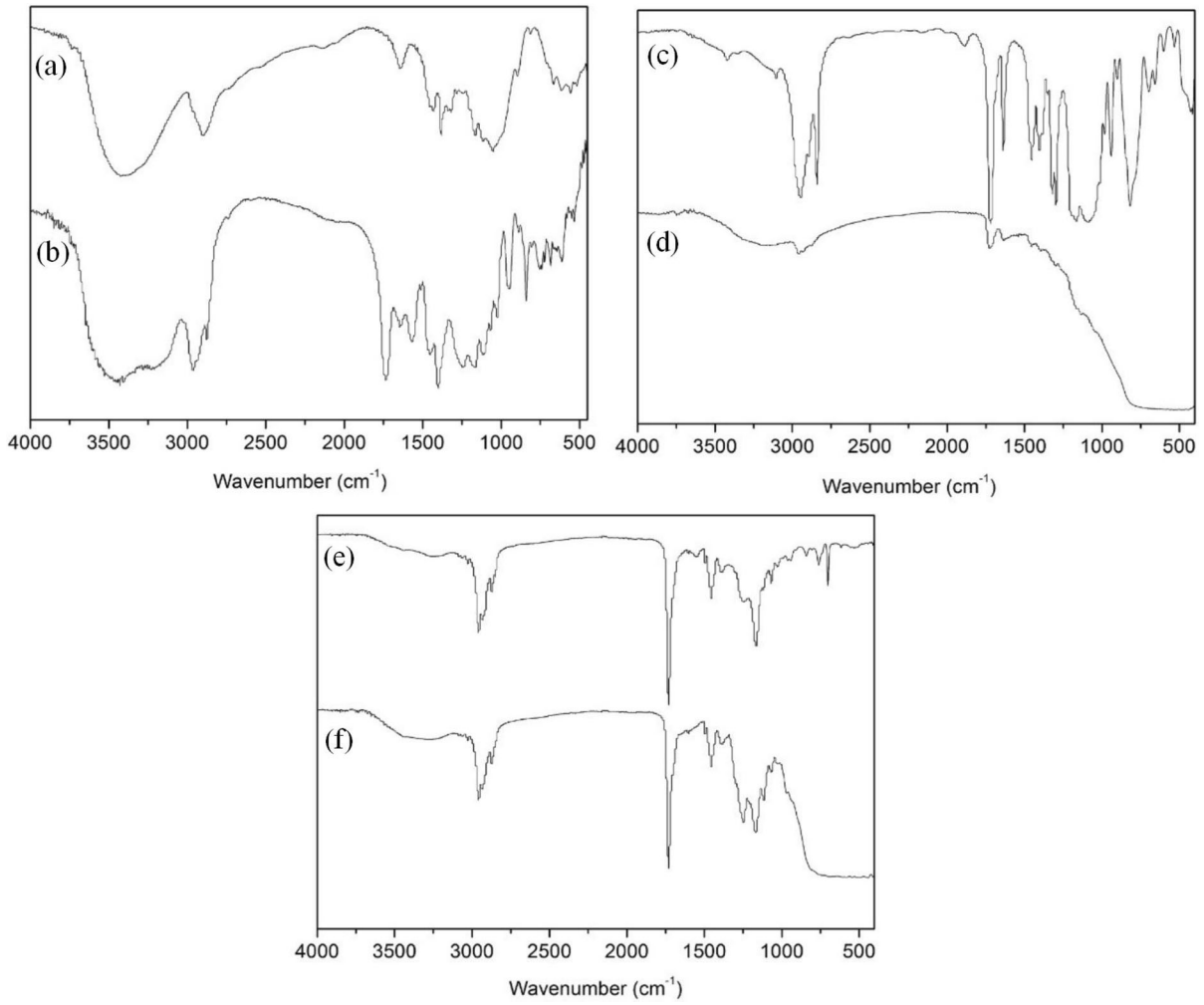

Fig. 5 FT-IR spectra of MCC (**a**), KH-570/MCC (**b**), KH-570 (**c**), KH-570/TiO_2 (**d**), Ti-0 (**e**), and Ti-4 (**f**)

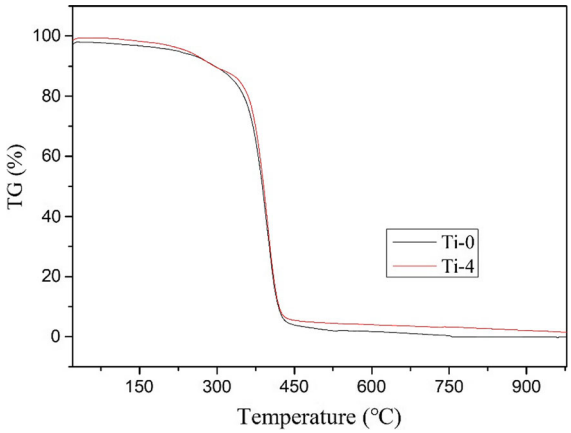

Fig. 6 TG curves of Ti-0 and Ti-4 films

with better thermal stability could enhance the heat resistance. The TG analysis showed that Ti-4 film had better thermal stability than that of Ti-0 and was more suitable for the paper cultural relic protection.

Dry heat accelerated aging test and reversibility experiment of protective coatings

According to the above analysis and discussion and considering the comprehensive properties, the Ti-4 material was preferred as the protective coatings for further experimental research.

To obtain the result of paper aging in a limited time, the dry heat accelerated aging test was conducted as a standard for evaluating the protective coatings. As shown in Table 4, after 72 h of aging test, the tensile

Table 4 The tensile strength retention rate (u), weight loss rate ($\triangle m$), tensile strength and average thickness of samples

Sample	u (%)			$\triangle m$ (%)			Tensile strength (N/m)	Average thickness (mm)
	24 h	48 h	72 h	24 h	48 h	72 h		
Sample-A	91.55	85.74	80.13	2.36	8.64	12.3	358.03	0.0742
Sample-B	96.34	93.69	91.08	2.48	3.14	3.48	1374.89	0.0815
Sample-C	/			/			342.17	0.0736

strength retention rate of Sample-A and Sample-B was 81.03% and 91.08%, respectively. The tensile strength of Sample-A and Sample-B had decreased, but the tensile strength retention rate of Sample-B was higher than that of Sample-A, indicating that the prepared Ti-4 coating could reduce the degree of dry heat aging damage to the paper.

The weight loss rate of paper samples after aging test is summarized in Table 4. The water content of Sample-B was higher than that of Sample-A because the surface of Sample-B was coated with Ti-4. Therefore, the weight loss rate of Sample-B was more than Sample-A after the 24 h aging test due to the moisture of samples was lost firstly. As the aging time increased, the weight loss rate of Sample-A increased significantly. After 72 h of the aging test, the weight loss rate of Sample-A was about 3.5 times that of Sample-B. This was because the gradual degradation of the main components (cellulose, hemicellulose, and lignin) in the paper. In contrast, the weight loss rate of Sample-B changed less due to the surface protective coating sealing.

For revealing the different appearance of Sample-A, Sample-B, and Sample-C, the surfaces of paper samples were recorded by photographs. The photographs of different paper samples are shown in Fig. 7. Figure 7a is a photo of the original Sample-A without protective coatings. From Fig. 7b, the coated protective coatings had high gloss and transparency, and hardly changed the sharpness of the writing on the paper and the appearance of the paper. Besides, as shown in Fig. 7c, the appearance of the paper, including the Chinese characters written on the paper, had no significant difference after the reversibility experiment, showing that the protective coatings had good reversibility and no damage to paper.

Water and oil were dropped onto the surface of the Sample-A and Sample-B to investigate the sealing effects of the protective coatings, and the results are shown in Fig. 7d, e. From Fig. 7d, water and oil dropped onto the surface of Sample-A would infiltrate the inside of the paper sample and gradually damage it. As shown in Fig. 7e, f, water and oil could not infiltrate to the inner of the Sample-B. After wiping off the water and oil on the surface of Sample-B with a filter paper, there was no noticeable change in appearance compared with the original Sample-B, suggesting that the Ti-4 coating could prevent water and oil pollution, mainly due to the self-cleaning ingredients such as DFMA and modified nano-TiO_2 contained in the protective coatings (Yang et al. 2014).

The protective coatings should be performed at the optimal thickness. The average value of sample thickness is listed in Table 4. Owing to the thickness of the Ti-4 coating film, the average thickness of Sample-B was increased by 0.0074 mm when compared to that of Sample-A. However, after the protective coatings were removed by the reversibility experiment, the thickness of the Sample-C was almost the same as that of the sample without the protective coatings (Sample-A). The results indicated that the protective coatings had good reversibility and had no effect on the paper thickness.

The average tensile strength of Samples-A, Sample-B and Sample-C was 358.03 N/m, 1374.89 N/m, and 342.17 N/m, respectively. Before and after coating the protective material, the considerable difference of tensile strength suggested that the mechanical properties of the paper sample were significantly improved by the Ti-4 coating. After the protective coatings were removed by reversibility experiment, the tensile strength was no difference between Sample-C and Sample-A, indicating that the reversibility experiment had little influence on the mechanical strength of the paper sample.

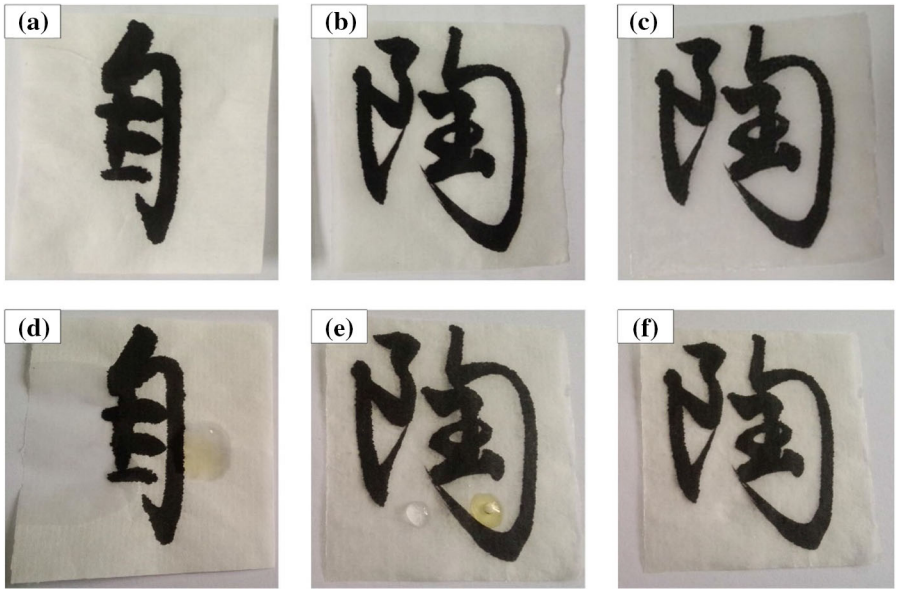

Fig. 7 The photos of Sample-A (**a**), Sample-B (**b**), Sample-C (**c**), water and oil dropped on Sample-A (**d**), water and oil dropped on Sample-B (**e**), and wiped off the water and oil on the Sample-B (**f**)

Scanning electron microscope (SEM) analysis

The morphological structures of paper samples are examined using SEM. Figure 8 shows the SEM images of different paper samples before and after treatments. Figure 8a is the image of the uncoated protective coating paper (Sample-A), indicating tightly packed fibers of cellulose with an interwoven network without any deformation, and there were some fine filaments connected between the coarse fibers. The surface structure of Sample-A after the aging test is shown in Fig. 8b. From Fig. 8b, some of the coarse fibers were broken, and most of the

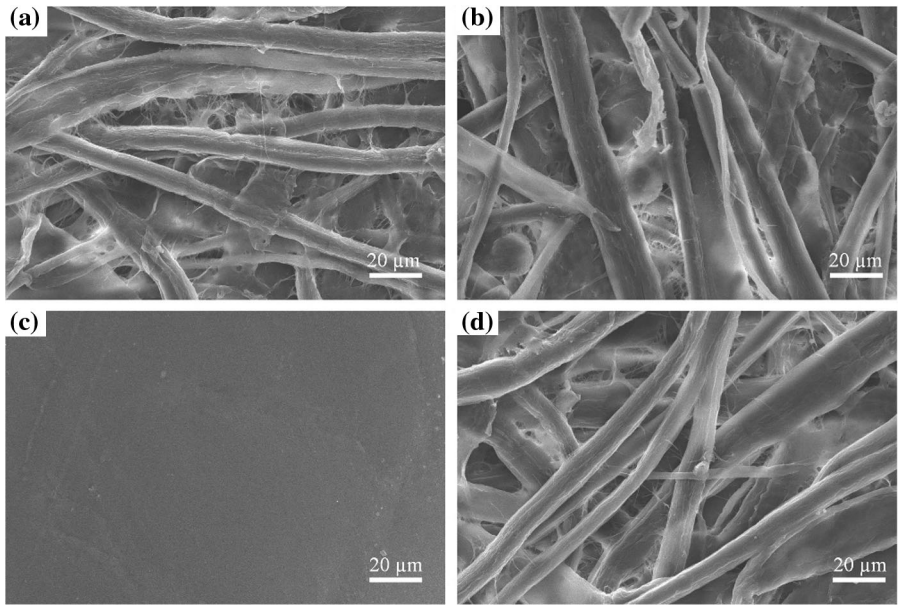

Fig. 8 SEM images of Sample-A (**a**), Sample-A after dry heat accelerated aging test (**b**), Sample-B (**c**), and Sample-C (**d**)

filamentous fibers formerly existing between the coarse fibers had disappeared. These observations showed that paper fibers might be damaged by the dry heat aging. As shown in Fig. 8c, it was evident that the Ti-4 emulsion exhibited good penetrability, having an excellent protective effect on the paper sample. After coating with the protective coatings, the surface of the paper samples was smooth, and some white points (modified nano-TiO_2 particles) were found in the image. The SEM image of the paper sample after reversibility experiment is shown in Fig. 8d. The fiber shape in the Sample-C was almost the same as that in the original Sample-A. Figure 8d shows that the protective Ti-4 coating had good reversibility and could protect the fibers in the paper well. Therefore, the prepared protective coatings conformed to the requirement for the paper cultural relic protection.

Conclusions

In this work, a simple polymerization method to prepare paper cultural relic protective coatings based on MCC, nano-TiO_2, DFMA, and several acrylate monomers was demonstrated. The protective coating emulsions exhibited good stability, lower viscosity and surface tension. The protective coating films showed good acid/alkali resistance, oil and water repellency, and good compatibility with the simulated paper cultural relics. The optimal amount of modified nano-TiO_2 was 1.0 wt% in this research. The dry heat accelerated aging test showed that the protective coatings could reduce the rate of aging. In addition, the reversibility experiment revealed that the protective coatings had the excellent reversible ability. After removing the protective coatings, the paper sample was very similar to the original paper in various performance parameters. Based on the above advantages, the MCC/TiO_2/F/SAE protective coatings had a positive effect on paper cultural relic protection.

Acknowledgments This work was financially supported by Society Development Fund of Zhenjiang (Grant No. SH2018009), 333 High-Level Personnel Training Project of Jiangsu Province (Grant No. BRA2016142), Qing Lan Project of Jiangsu Province (2018-2021), National Natural Science Foundation of China (Grant No. 21706100), "169 Project" of Zhenjiang City (2016-2020) and Zhenjiang College Scientific Research Team (Grant No. ZJCKYTD2017023).

References

Afsharpour M, Hadadi M (2014) Titanium dioxide thin film: environmental control for preservation of paper-art-works. J Cult Herit 15:569–574. https://doi.org/10.1016/j.culher.2013.10.008

Ashori A, Nourbakhsh A (2010) Performance properties of microcrystalline cellulose as a reinforcing agent in wood plastic composites. Compos Part B-Eng 41:578–581. https://doi.org/10.1016/j.compositesb.2010.05.004

Bicchieri M, Sodo A (2016) Alcoholic deacidification and simultaneous deacidification-reduction of paper evaluated after artificial and natural aging. J Cult Herit 20:599–606. https://doi.org/10.1016/j.culher.2016.02.008

Chen Q, Wen W, Qiu F, Xu J, Yu H, Chen M, Yang D (2016) Preparation and application of modified carboxymethyl cellulose Si/polyacrylate protective coating material for paper relics. Chem Pap 70:946–959. https://doi.org/10.1515/chempap-2016-0029

Giolando DM (2016) Transparent self-cleaning coating applicable to solar energy consisting of nano-crystals of titanium dioxide in fluorine doped tin dioxide. Sol Energy 124:76–81. https://doi.org/10.1016/j.solener.2015.11.024

Jun SH, Lee SH, Kim S, Park SG, Lee CK, Kang NK (2017) Physical properties of TEMPO-oxidized bacterial cellulose nanofibers on the skin surface. Cellulose 24:5267–5274. https://doi.org/10.1007/s10570-017-1508-2

Kalu OI, Subramanian B, MacLean BJ, Saha GC (2019) A novel approach to the sol-gel synthesis of titanium dioxide-coated SBA-16 type silica mesoporous microspheres for water purification. Materialia 5:100237. https://doi.org/10.1016/j.mtla.2019.100237

Kim Y, Hong J, Jo C, Kim S, Lee J, Choi K (2015) Effects of asarum sieboldii miquel extracts on the properties of Korean traditional paper (Hanji). J Cult Herit 16:890–895. https://doi.org/10.1016/j.culher.2015.02.004

Li Q, Xi S, Zhang X (2014a) Conservation of paper relics by electrospun PVDF fiber membranes. J Cult Herit 15:359–364. https://doi.org/10.1016/j.culher.2013.09.003

Li Q, Xi S, Zhang X (2014b) Deacidification of paper relics by plasma technology. J Cult Herit 15:159–164. https://doi.org/10.1016/j.culher.2013.03.004

Li P, Qiu F, Zhang X, Wang L, Chen Q, Yang D (2015) Preparation and application of fluorinated-siloxane protective surface coating material for stone inscriptions. J Polym Eng 35:511–522. https://doi.org/10.1515/polyeng-2014-0266

Li J, Liu X, Zheng Q, Chen L, Huang L, Ni Y, Ouyang X (2019) Urea/NaOH system for enhancing the removal of hemicellulose from cellulosic fibers. Cellulose 26:6393–6400. https://doi.org/10.1007/s10570-019-02587-7

Liu L, Zhang L, Zhang B, Hu Y (2019) A comparative study of reinforcement materials for waterlogged wood relics in laboratory. J Cult Herit 36:94–102. https://doi.org/10.1016/j.culher.2018.08.002

López-Zamora L, Martínez-Martínez HN, González-Calderón JA (2018) Improvement of the colloidal stability of titanium dioxide particles in water through silicon based coupling agent. Mater Chem Phys 217:285–290. https://doi.org/10.1016/j.matchemphys.2018.06.063

MacFarlane JW, Jenkinson HF, Scott TB (2011) Sterilization of microorganisms on jet spray formed titanium dioxide surfaces. Appl Catal B-Environ 106:181–185. https://doi.org/10.1016/j.apcatb.2011.05.023

Melo D, Sequeira SO, Lopes JA, Macedo MF (2019) Stains versus colourants produced by fungi colonising paper cultural heritage: a review. J Cult Herit 35:161–182. https://doi.org/10.1016/j.culher.2018.05.013

Pfendler S, Karimi B, Alaoui-Sosse L, Bousta F, Alaoui-Sossé B, Abdel-Daim MM, Aleya L (2019) Assessment of fungi proliferation and diversity in cultural heritage: reactions to UV-C treatment. Sci Total Environ 647:905–913. https://doi.org/10.1016/j.scitotenv.2018.08.089

Purcar V, Rădiţoiu V, Dumitru A, Nicolae C, Frone A, Anastasescu M, Rădiţoiu A, Raduly M, Gabor R, Căprărescu S (2019) Antireflective coating based on TiO_2 nanoparticles modified with coupling agents via acid-catalyzed sol-gel method. Appl Surf Sci 487:819–824. https://doi.org/10.1016/j.apsusc.2019.02.256

Qiu Z, Shi S, Qiu F, Xu X, Yang D, Zhang T (2020) Enhanced As(Ⅲ) removal from aqueous solutions by recyclable Cu@MNM composite membranes via synergistic oxidation and absorption. Water Res 168:115147. https://doi.org/10.1016/j.watres.2019.115147

Sterflinger K (2010) Fungi: their role in deterioration of cultural heritage. Fungal Biol Rev 24:47–55. https://doi.org/10.1016/j.fbr.2010.03.003

Sun C, Dai J, Zhang H, Zhang F, Zhang N (2019) Preparation and characterization of spherical titania and their influence on self-cleaning and anticorrosion properties of acrylic resin. Prog Org Coat 128:21–31. https://doi.org/10.1016/j.porgcoat.2018.12.005

Wang B, Duan Y, Zhang J (2016) Titanium dioxide nanoparticles-coated aramid fiber showing enhanced interfacial strength and UV resistance properties. Mater Des 103:330–338. https://doi.org/10.1016/j.matdes.2016.04.085

Wang Y, An Q, Yang B (2019) Synthesis of UV-curable polyurethane acrylate modified with polyhedral oligomeric silsesquioxane and fluorine for iron cultural relic protection coating. Prog Org Coat 136:105235. https://doi.org/10.1016/j.porgcoat.2019.105235

Xu J, Jiang Y, Qiu F, Dai Y, Yang D, Yu Z, Yang P (2018a) Synthesis, mechanical properties and iron surface conservation behavior of UV-curable waterborne polyurethane-acrylate coating modified with inorganic carbonate. Polym Bull 75:4713–4734. https://doi.org/10.1007/s00289-018-2294-1

Xu J, Jiang Y, Qiu F, Dai Y, Yang D, Yu Z, Yang P (2018b) Fabrication of UV-curable waterborne fluorinated polyurethane-acrylate and its application for simulated iron cultural relic protection. J Coat Technol Res 15:535–541. https://doi.org/10.1007/s11998-017-0009-4

Xu J, Zhang T, Jiang Y, Yang D, Qiu F, Chen Q, Yu Z (2020a) Preparation of self-healing acrylic copolymer composite coatings for application in protection of paper cultural relics. Polym Eng Sci 60:288–296. https://doi.org/10.1002/pen.25282

Xu J, Zhang T, Zhang X, Jiang Y, Yang D, Qiu F, Yu Z (2020b) Preparation of polymeric material containing UV absorber for application in paper-based relics protection. Polym-Plast Technol Eng 59:536–545. https://doi.org/10.1080/25740881.2019.1669651

Yang X, Zhu L, Zhang Y, Chen Y, Bao B, Xu J, Zhou W (2014) Surface properties and self-cleaning ability of the fluorinated acrylate coatings modified with dodecafluoroheptyl methacrylate through two adding ways. Appl Surf Sci 295:44–49. https://doi.org/10.1016/j.apsusc.2013.12.177

Yang F, Zhu L, Han D, Cao R, Li W, Chen Y, Wang X, Ning L (2016) Preparation and failure behavior of fluorine-containing acrylic polyurethane coating. Prog Org Coat 90:455–462. https://doi.org/10.1016/j.porgcoat.2015.11.009

Zervos S, Alexopoulou I (2015) Paper conservation methods: a literature review. Cellulose 22:2859–2897. https://doi.org/10.1007/s10570-015-0699-7

Zhang X, Wen W, Yu H, Chen Q, Xu J, Yang D, Qiu F (2016a) Preparation and artificial ageing tests in stone conservation of fluorosilicone vinyl acetate/acrylic/epoxy polymers. Chem Pap 70:1621–1631. https://doi.org/10.1515/chempap-2016-0095

Zhang X, Wen W, Yu H, Qiu F, Chen Q, Yang D (2016b) Preparation, characterization of nano-silica/fluoroacrylate material and the application in stone surface conservation. J Polym Res 23:75. https://doi.org/10.1007/s10965-016-0967-8

Zhang T, Yuan D, Guo Q, Qiu F, Yang D, Ou Z (2019) Preparation of a renewable biomass carbon aerogel reinforced with sisal for oil spillage clean-up: inspired by green leaves to green Tofu. Food Bioprod Process 114:154–162. https://doi.org/10.1016/j.fbp.2018.12.007